Covariant kaon dynamics and kaon flow in heavy ion collisions

Yu-Ming Zheng
China Institute of Atomic Energy, P.O. Box 275(18), Beijing 102413, People's Republic of China

C. Fuchs, Amand Faessler, and K. Shekhter
Institut für Theoretische Physik der Universität Tübingen, D-72076 Tübingen, Germany

Yu-Peng Yan and Chinorat Kobdaj
School of Physics, Suranarre University of Technology, Nakhon Ratchasima 30000, Thailand
(Received 2 December 2002; revised manuscript received 22 December 2003; published 25 March 2004)

The influence of the chiral mean field on the K^+ transverse flow in heavy ion collisions at SIS energy is investigated within covariant kaon dynamics. For the kaon mesons inside the nuclear medium a quasiparticle picture including scalar and vector fields is adopted and compared to the standard treatment with a static potential. It is confirmed that a Lorentz force from spatial component of the vector field provides an important contribution to the in-medium kaon dynamics and strongly counterbalances the influence of the vector potential on the K^+ in-plane flow. The FOPI data can be reasonably described using in-medium kaon potentials based on effective chiral models. The information on the in-medium K^+ potential extracted from kaon flow is consistent with the knowledge from other sources.

DOI: 10.1103/PhysRevC.69.034907 PACS number(s): 25.75.Ld, 24.10. Jv, 25.75.Dw

I. INTRODUCTION

Properties of kaons in dense hadronic matter are important for a better understanding of both, a possible restoration of chiral symmetry in dense hadronic matter and the properties of nuclear matter at high densities. It is known from chiral models that the kaon mean field is related to chiral symmetry breaking [1]. The in-medium effects give rise to an attractive scalar potential inside the nuclear medium which is in mean-field approximation proportional to the kaon-nucleon sigma term Σ_{KN}. A second part of the mean field originates from the interaction with vector mesons [1–5]. The vector potential is repulsive for kaons K^+ and, due to G-parity conservation, attractive for antikaons K^-. A strong attractive potential for antikaons may also favor K^- condensation at high nuclear densities and thus modifies the properties of neutron stars [6].

There have been extensive experimental efforts to search for the kaon in-medium properties in heavy ion collisions, in particular at intermediate energies [7–11]. Corresponding transport calculations revealed significant evidence for in-medium modifications of the kaon properties during the course of such reactions [12–21]. The picture was recently complemented by the measurements of K^+ production in proton-nucleus reactions at COSY-ANKE [22]. While $A+A$ reactions test the kaon dynamics also at supranormal nuclear densities, $p+A$ reactions cannot exceed saturation density. However, in the latter case the reaction dynamics is theoretically much easier to handle (due to much less secondary scatterings) and therefore the interpretation of the data is more straightforward. From the $p+A$ data the existence of a repulsive in-medium K^+ potential of about 20 MeV at saturation density $[U_K(\rho_0) \simeq 20\ \mathrm{MeV}]$ was derived [22].

In $A+A$ reactions the transverse flow of K^+ mesons is one of the specially attractive observables. It was proposed by Ko and Li [12] that the kaon flow pattern at the final stage can be used as a sensitive probe for the kaon potential in a nuclear medium. Other theoretical studies predicted similar features for the kaon flow [14,18]. As pointed out by Fuchs *et al.* [19], however, the kaon dynamics used in the above investigations is noncovariant, i.e., it is based on a static potential-like force. The Lorentz-force-like contribution from a typical relativistic scalar-vector-type structure is missing. However, this contribution strongly counterbalances the influence of the vector potential on the K^+ in-plane flow which makes it more difficult to draw definite conclusions from transverse flow pattern.

In the meantime the FOPI Collaboration [23] published new data of K^+ side flow with improved precision. These open the possibility to study this problem in more detail. In this work we apply the covariant kaon dynamics to describe the kaon in-medium properties, discuss its influence on the K^+ in-plane flow in heavy ion collisions, and compare to the standard treatment with a static potential. Our studies show that a relatively strong repulsive K^+ potential as proposed by Brown and Rho can reproduce the new FOPI data in the covariant kaon dynamics quite well and the strength of the potential is roughly consistent with recent information obtained from $p+A$ scattering [22].

II. THE MODEL

Due to its relativistic origin, the kaon mean field has a typical relativistic scalar-vector-type structure. For the nucleons such a structure is well known from Quantum Hadron Dynamics [24]. This decomposition of the mean field is most naturally expressed by an absorption of the scalar and vector parts into effective masses and momenta, respectively, leading to a formalism of quasifree particles inside the nuclear medium [24].

From the chiral Lagrangian the field equations for the $K^{\pm}$ mesons are derived from the Euler-Lagrange equations [12]

$$\left[\partial_\mu\partial^\mu \pm \frac{3i}{4f_\pi^{*2}} j_\mu \partial^\mu + \left(m_K^2 - \frac{\Sigma_{KN}}{f_\pi^{*2}}\rho_s\right)\right]\phi_{K^\pm}(x) = 0. \quad (1)$$

Here the mean-field approximation has already been applied. In Eq. (1) ρ_s is the baryon scalar density, j_μ is the baryon four-vector current, f_π^* is the in-medium pion decay constant. Introducing the kaonic vector potential

$$V_\mu = \frac{3}{8f_\pi^{*2}} j_\mu, \quad (2)$$

Eq. (1) can be rewritten in the form [19]

$$[(\partial_\mu \pm iV_\mu)^2 + m_K^{*2}]\phi_{K^\pm}(x) = 0. \quad (3)$$

Thus, the vector field is introduced by minimal coupling into the Klein-Gordon equation. The effective mass m_K^* of the kaon is then given by [3,19–21,25]

$$m_K^* = \sqrt{m_K^2 - \frac{\Sigma_{KN}}{f_\pi^{*2}}\rho_s + V_\mu V^\mu}. \quad (4)$$

Due to the bosonic character, the coupling of the scalar field to the mass term is no longer linear as for the baryons but quadratic and contains an additional contribution originating from the vector field. The effective quasiparticle mass defined by Eq. (4) is a Lorentz scalar and is equal for K^+ and K^-. In nuclear matter at rest the spatial components of the vector potential vanish, i.e., $\mathbf{V}=0$, and Eq. (3) reduces to the expression already given in Ref. [12]. However, Eq. (3) generally account for the correct Lorentz properties which are not obvious from the standard treatment of the kaon mean field [12–14,6].

The covariant equations of motion are obtained in the classical (testparticle) limit from the relativistic transport equation for the kaons which can be derived from Eq. (3). They are analogous to the corresponding relativistic equations for baryons and read [19]

$$\frac{dq^\mu}{d\tau} = \frac{k^{*\mu}}{m_K^*}, \quad \frac{dk^{*\mu}}{d\tau} = \frac{k_\nu^*}{m_K^*}F^{\mu\nu} + \partial^\mu m_K^*. \quad (5)$$

Here $q^\mu=(t,\mathbf{q})$ are the coordinates in Minkowski space and $F^{\mu\nu}=\partial^\mu V^\nu - \partial^\nu V^\mu$ is the field strength tensor for K^+. For K^- where the vector field changes sign. The equation of motion are identical, however, $F^{\mu\nu}$ has to be replaced by $-F^{\mu\nu}$. The structure of Eqs. (5) may become more transparent considering only the spatial components

$$\frac{d\mathbf{k}^*}{dt} = -\frac{m_K^*}{E^*}\frac{\partial m_K^*}{\partial \mathbf{q}} \mp \frac{\partial V^0}{\partial \mathbf{q}} \pm \frac{\mathbf{k}^*}{E^*} \times \left(\frac{\partial}{\partial \mathbf{q}} \times \mathbf{V}\right), \quad (6)$$

where the upper (lower) signs refer to K^+ (K^-). The term proportional to the spatial component of the vector potential gives rise to a momentum dependence which can be attributed to a Lorentz force, i.e., the last term in Eq. (6). Such a velocity dependent ($\mathbf{v}=\mathbf{k}^*/E^*$) Lorentz force is a genuine feature of relativistic dynamics as soon as a vector field is involved.

If the equations of motion are, however, derived from a static potential

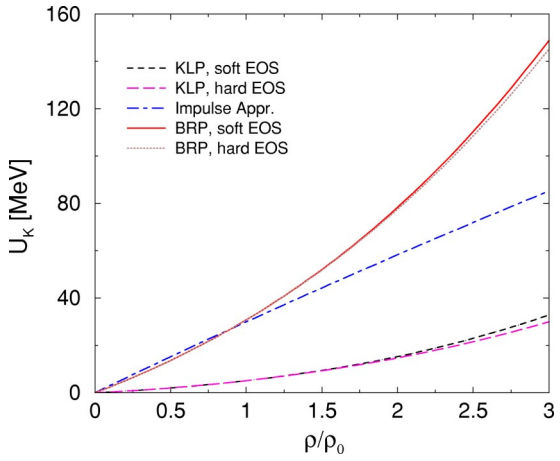

FIG. 1. (Color online) Density dependence of the in-medium kaon potential at zero momentum. The KLP and BRP stand for the Ko and Li parametrization and Brown and Rho parametrization, respectively.

$$U(\rho,\mathbf{k}) = \omega(\rho,\mathbf{k}) - \omega_0(\mathbf{k}) = \sqrt{\mathbf{k}^2 + m_K^2 - \frac{\Sigma_{KN}}{f_\pi^{*2}}\rho_s + V_0^2} \pm V_0 - \sqrt{\mathbf{k}^2 + m_K^2} \quad (7)$$

as given in Refs. [6,12–14,18], the Lorentz-force (LF)-like contribution is missing. Noncovariant treatments are formulated in terms of canonical momenta k instead of kinetic momenta k^* and then the equations of motion read

$$\frac{d\mathbf{k}}{dt} = -\frac{m_K^*}{E^*}\frac{\partial m_K^*}{\partial \mathbf{q}} \mp \frac{\partial V^0}{\partial \mathbf{q}} \pm \mathbf{v}_i\frac{\partial \mathbf{V}_i}{\partial \mathbf{q}}, \quad (8)$$

where $\mathbf{v}=\mathbf{k}^*/E^*$ the kaon velocity.

Following Brown and Rho [2], we use $\Sigma_{KN}=450$ MeV, $f_\pi^{*2}=0.6f_\pi^2$ for the vector field and $f_\pi^{*2}=f_\pi^2$ for the scalar part given by $-\Sigma_{KN}/f_\pi^{*2}\rho_s$. This accounts for the fact that the enhancement of the scalar part using f_π^{*2} is compensated by higher-order corrections in the chiral expansion [2,4]. This parametrization is denoted as Brown and Rho parametrization (BRP), which has already been used in our previous investigations [19–21,25]. For comparison also a weaker potential with $\Sigma_{KN}=350$ MeV and $f_\pi^{*2}=f_\pi^2$ is applied. This parametrization was originally used in Ref. [12] and is called the Ko and Li parametrization (KLP) in the following. The baryon dynamics are treated within the framework of quantum molecular dynamics (QMD). For the nuclear forces we use the standard momentum dependent Skyrme interactions corresponding to a soft/hard equation of state (EOS) ($K=200/380$ MeV). For the determination of the kaon mean field we adopt the corresponding covariant scalar-vector description of the nonlinear $\sigma\omega$ model. Here we use the parametrizations of Refs. [13,26] which correspond to identical soft/hard nuclear EOSs.

The potentials given in Eq. (7) at zero momentum by the BRP and KLP are shown in Fig. 1, where one also shows the kaon potential determined from the kaon-nucleon scattering length using the impulse approximation (IA) [27]. In IA the energy $\omega(\rho,\mathbf{k})$, Eq. (7), is given as follows:

$$\omega(\rho,\mathbf{k}) = \sqrt{\mathbf{k}^2 + m_{\mathrm{K}}^2 - 4\pi\left(1+\frac{m_K}{m_N}\right)\overline{a}_{\mathrm{KN}}\rho}, \tag{9}$$

where m_N is the nucleon mass and $\overline{a}_{\mathrm{KN}} \approx -0.255$ fm is the isospin-averaged kaon-nucleon scattering length in free space [28]. It is seen from Fig. 1 that the potentials predicted by BRP with the soft equation of state (solid curve) and by KLP with soft EOS (dashed line) are slightly stronger than those with the hard EOS (see the dot curve and long-dashed line, respectively). Up to saturation density the impulse approximation and the BR potential almost coincide $[U_K(\rho_0) \simeq 30$ MeV] but at supranormal densities the BR potential rises much steeper than the IA. The KL potential $[U_K(\rho_0) \simeq 5$ MeV, dashed line], on the other hand, is much weaker than those given by both, BRP and IA.

The K^+ creation mechanism is treated as described in Refs. [20,21,25] where one uses the improved cross section of Refs. [29,30] for the baryon induced K^+ creation channels and of Ref. [31] for the pion induced channels. The kaon production is treated perturbatively and does generally not affect the reaction dynamics [13,20,21,25,26]. The shift of the production thresholds of the kaons by the in-medium potentials are taken into account as described in Refs. [20,21,25]. In order to account for energy-momentum conservation it is useful to formulate the mass-shell condition, Eq. (3), in terms of the canonical momenta

$$0 = k_\mu^{*2} - m_{\mathrm{K}}^{*2} = k_\mu^2 - m_{\mathrm{K}}^2 - 2m_{\mathrm{K}}U_{\mathrm{opt}} \tag{10}$$

with

$$U_{\mathrm{opt}}(\rho,\mathbf{k}) = -\Sigma_S + \frac{1}{m_{\mathrm{K}}}k_\mu V^\mu + \frac{\Sigma_S^2 - V_\mu^2}{2m_{\mathrm{K}}}. \tag{11}$$

Here we introduced the total scalar kaon self-energy $\Sigma_S = m_{\mathrm{K}}^* - m_{\mathrm{K}}$. Since U_{opt} is a Lorentz scalar it can also be absorbed into an effective mass

$$\tilde{m}_{\mathrm{K}}(\rho,\mathbf{k}) = \sqrt{m_{\mathrm{K}}^2 + 2m_{\mathrm{K}}U_{\mathrm{opt}}(\rho,\mathbf{k})} \tag{12}$$

which sets the canonical momenta on the mass-shell

$$0 = k_\mu^{*2} - m_{\mathrm{K}}^{*2} = k_\mu^2 - \tilde{m}_{\mathrm{K}}^2. \tag{13}$$

By definition $\tilde{m}_{\mathrm{K}}$ is a scalar but in contrast to m_{K}^* who's analog is the Dirac mass in the case of nucleons $\tilde{m}_{\mathrm{K}}$ absorbs the full optical potential and corresponds at zero momentum to the energy ω. The threshold condition for K^+ production in baryon induced reactions reads then

$$\sqrt{s} \geqslant \tilde{m}_B + \tilde{m}_Y + \tilde{m}_K, \tag{14}$$

where $\sqrt{s}$ is the center-of-mass energy of the colliding baryons. The momenta of the outgoing particles are distributed according to the three-body phase space

$$d\Phi_3(\sqrt{s},\tilde{m}_B,\tilde{m}_Y,\tilde{m}_K) = d\Phi_2(\sqrt{s},\tilde{m}_B,M)dM^2\Phi_2(M,\tilde{m}_Y,\tilde{m}_K). \tag{15}$$

The two-body phase space in Eq. (15) has the form

$$\Phi_2(\sqrt{s},m_1,m_2) = \frac{\pi p^*(\sqrt{s},m_1,m_2)}{\sqrt{s}}, \tag{16}$$

where

$$p^*(\sqrt{s},m_1,m_2) = \frac{\sqrt{(s-(m_1+m_2)^2)(s-(m_1-m_2)^2)}}{2\sqrt{s}} \tag{17}$$

is the momentum of the particles 1 and 2 in the center of mass (c.m.) frame. Equation (15) corresponds to a distribution of the particle momenta according to an isotropic three-body phase space. However, in Ref. [6] a parametrization of the form

$$d\Phi_3(\sqrt{s},\tilde{m}_B,\tilde{m}_Y,\tilde{m}_K) = dW_K(\sqrt{s},\tilde{m}_B,\tilde{m}_Y,M_K)dM_K^2\Phi_2(\sqrt{s}-M_K,\tilde{m}_Y,\tilde{m}_B) \tag{18}$$

has been suggested where the kaon momentum p is distributed according to

$$dW_K \simeq \left(\frac{p}{p_{\max}}\right)^3\left(1-\frac{p}{p_{\max}}\right)^2, \tag{19}$$

with $p_{\max} = p^*(\sqrt{s},\tilde{m}_B+\tilde{m}_Y,\tilde{m}_K)$ the maximal kaon momentum in the BB c.m. frame. $M_K = \sqrt{p^2+\tilde{m}_K^2}$ in Eq. (18). The parametrization of Eq. (18) has been motivated by analyzing corresponding $pp \to p\Lambda K^+$ data [6] and shifts the kaon spectrum to lower momenta compared to an ideal three-body phase space. The optical potentials of the baryons which enter via $\tilde{m}_B, \tilde{m}_Y$ are taken from the soft/hard EOS versions of the $\sigma\omega$ model [13,26]. The hyperon fields are thereby scaled according to SU(3) symmetry $U_{\mathrm{opt}}^Y = \frac{2}{3}U_{\mathrm{opt}}^B$. Since the $\tilde{m}$'s depend on the final state momenta the determination of $d\Phi_3$ is a self-consistency problem which is solved by iteration. The same procedure is applied to the two-body-phase space in pion induced reactions. The rescattering of the K^+ mesons with baryons and the Coulomb interaction are taken into account. The electromagnetic interaction is treated analogously to the strong interaction, i.e., by adding $F_{\mathrm{el}}^{\mu\nu} = \partial^\mu A^\nu - \partial^\nu A^\mu$ given by the electromagnetic vector potential to Eq. (5).

III. RESULTS

In order to study first the influence of the three-body phase space in BB collisions we consider in Fig. 2 $C+C$ collisions at 2.0A GeV. The KaoS Collaboration has measured inclusive K^+ spectra at various c.m. angles with high precision. Corresponding calculations are performed with the soft EOS including the K^+ in-medium potential BRP and final state interactions by rescattering processes. In this scenario the excitation function of the kaon multiplicities measured by KaoS [10] is well reproduced over a large energy range from 0.8 to 2 A GeV [20]. Without in-medium potentials the total multiplicities are significantly overpredicted. Looking to the spectra in more detail we find that an isotropic three-body phase space in the $BB \to BY\,K^+$ channel shifts the spectra to too high momenta. The empirical parametriza-

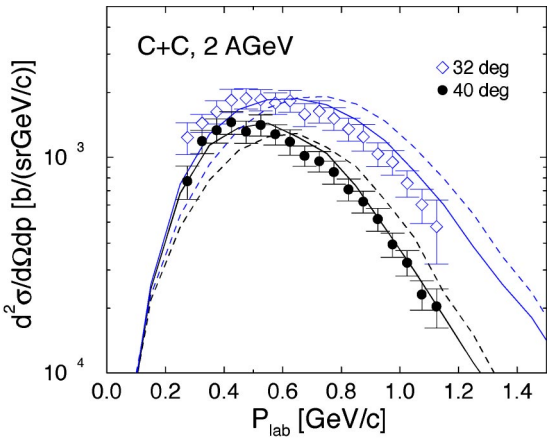

FIG. 2. (Color online) Inclusive K^+ spectra at $\theta_{lab}=32°,40°$ in $^{12}C+^{12}C$ reactions at 2.0A GeV. The calculations are performed using different descriptions of the $BB\rightarrow BYK^+$ final state three-body phase space. The dotted curves refer to an isotropic three-body phase space, while the solid curves are obtained using the parametrization of Eq. (19) with an additional empirical c.m. angular anisotropy (see text). The corresponding KaoS data are taken from Ref. [32].

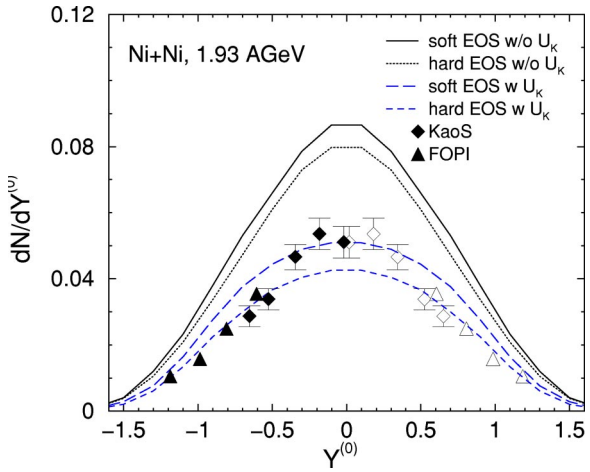

FIG. 3. (Color online) K^+ rapidity distributions in 1.93A GeV $^{58}Ni+^{58}Ni$ reactions at impact parameter $b\leqslant 4$ fm. The calculations are performed with and without the BRP K^+ in-medium potential and using a soft/hard EOS. Diamonds represent data from KaoS [9], triangles those from FOPI [11].

tion of the three-body phase space suggested in Ref. [6], Eq. (17), improves the situation but is still not fully sufficient to account for the angular asymmetry which is seen in the KaoS data [32]. A relatively good agreement can be achieved introducing an empirical angular dependence $d\sigma\propto(1+a\cos^2\theta_{c.m.})d\cos\theta_{c.m.}$ in the elementary cross sections. Following the data analysis of [32] an asymmetry parameter $a=1.2$ leads to slightly forward/backward peaked elementary $BB\rightarrow BY\,K^+$ cross sections and the corresponding spectra shown in Fig. 2 are then well reproduced by the transport calculations.

In order to investigate the influence of covariant dynamics on the K^+ in-plane flow we consider the 1.93A GeV $^{58}Ni+^{58}Ni$ collisions at impact parameter $b\leqslant 4$ fm, corresponding to the FOPI centrality cut. The K^+ rapidity distributions dN/dY^0 ($Y^0=Y_{lab}/Y_{CM}-1$) for this reaction is shown in Fig. 3. Again the BRP in-medium kaon potential has been used. Consistent with our previous results [20] and those from other groups [16], this figure shows that the existence of a repulsive kaon potential is required to match the experimental data [9,11], in particular around midrapidity. The influence of the nuclear EOS is thereby on the 20% level. The best agreement with the data is obtained with the soft EOS and including a kaon potential.

The next figure (Fig. 4) gives the corresponding proton flow. A p_t cut of $p_t/m>0.5$ accounts for the experimental acceptance [7,23]. At this high energy the dependence of the proton flow on the nuclear EOS is weak and both options, i.e., a soft and a hard EOS reproduce the FOPI data [7] reasonably well. It should be noted that the analysis has been performed for all protons. At large rapidities the experimental flow is rather well reproduced whereas deviations occur between $-1\leqslant Y^0\leqslant 0$ where the consideration of cluster effects might help to improve on the data fitting. It is, on the other hand, known from Ref. [15] that proton and kaon flow are only very loosely connected. The kaon producing sources carry this large in-plane flow. The kaons themselves carry a much smaller flow fraction since, at a given rapidity, they are produced from two baryons originating from very different rapidity regions. Therefore baryon sources with positive and negative p_x/m values add up to an almost vanishing net flow (see the results given by open down triangles in Fig. 5). Λ's which are produced in association with K^+'s have very similar flow pattern as protons, i.e., they show almost the same p_x/m scaling [23]. In Ref. [33] the Λ flow was investigated within the present model and the data were best reproduced including the hyperon mean field according to SU(3) scaling $U^Y_{opt}=\frac{2}{3}U^B_{opt}$. As also observed in Ref. [34] the primordial Λ flow is moderate but strongly enhanced by the ΛN final state interactions, i.e., rescattering and the mean field.

Figure 6 shows now the K^+ transverse flow as a function

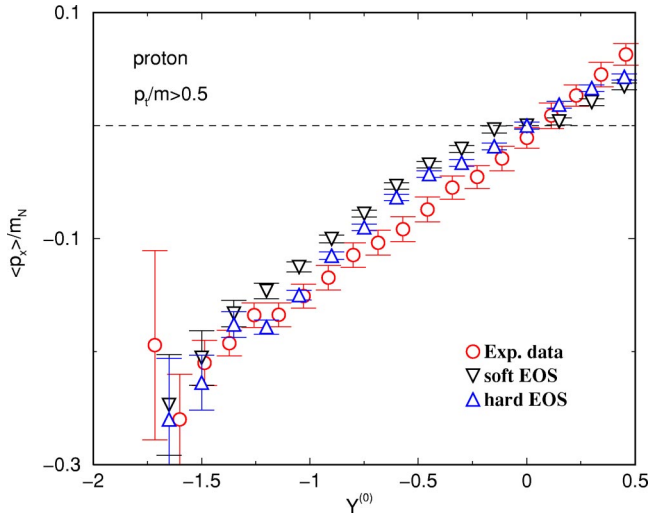

FIG. 4. (Color online) Transverse proton flow as a function of rapidity Y^0 in 1.93A GeV $^{58}Ni+^{58}Ni$ reactions at impact parameter $b\leqslant 4$ fm. The calculations with a soft ($\triangledown$) and hard ($\triangle$) nuclear EOS are compared to the FOPI data [7].

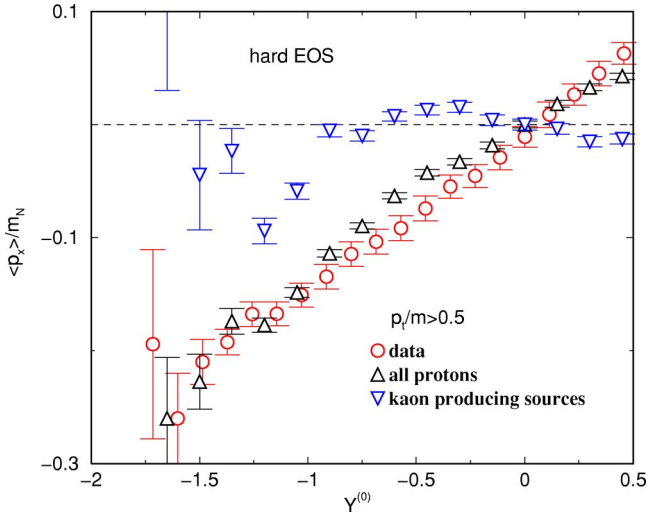

FIG. 5. (Color online) Transverse flow of the kaon producing sources as a function of rapidity Y^0 in 1.93A GeV ^{58}Ni+^{58}Ni reactions at impact parameter $b \leqslant 4$ fm. The calculations are performed with the BRP K^+ in-medium potential and using a hard nuclear EOS. The FOPI data are from Ref. [7].

of the scaled rapidity in 1.93A GeV ^{58}Ni+^{58}Ni reactions. In this figure the full squares represent the '95 data set from FOPI (old data) [7]. The full circles show the '99 data from FOPI [23] with improved statistics, open circles indicate their reflection at midrapidity. The theoretical results are given by the BRP with a soft EOS. Around midrapidity the two calculations with U_K&LF (static potential + Lorentz force, open down triangles) and without U_K (open up triangles) almost coincide. The result without U_K, i.e., only including the kaon rescattering effect, predicts a slightly positive flow. The result with U_K&LF leads to a very small

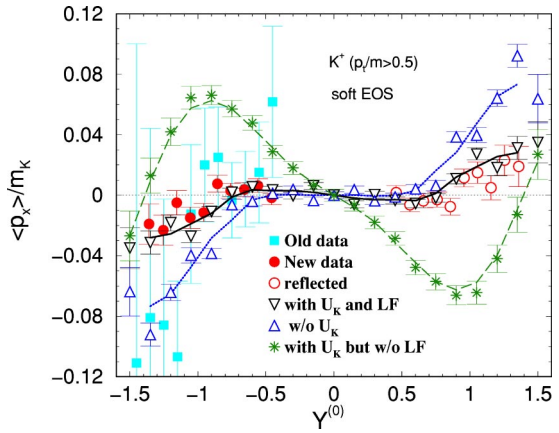

FIG. 6. (Color online) The K^+ transverse flow as a function of rapidity Y^0 in 1.93A GeV ^{58}Ni+^{58}Ni reactions at impact parameter $b \leqslant 4$ fm. The calculations are performed using the BRP K^+ in-medium potential with a soft EOS. The full squares represent the FOPI data from Ref. [7], full circles are more recent FOPI data [23], their reflections with respect to midrapidity are shown by the open circles. The open down triangles denote the calculated results with U_K and the Lorentz-force (LF) contribution. The open up triangles indicate the results without U_K. The stars stand for the results with U_K but without LF.

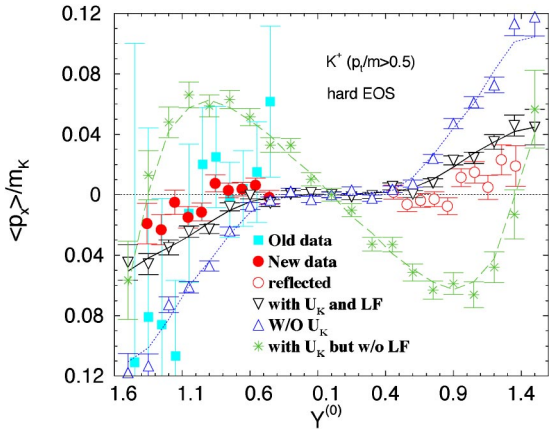

FIG. 7. (Color online) Same as shown in Fig. 6, but with a hard EOS.

antiflow. Around midrapidity both calculations agree with the data within error bars. However, at spectator rapidities the two results with U_K&LF and without U_K differ substantially from each other. With respect to the old data set both calculations, i.e., with U_K&LF and without U_K, agree with experiment within error bars since both reproduce the nearly vanishing side flow signal of K^+'s around midrapidity. This means that the old data can be reproduced without need for an in-medium kaon potential [15]. However, the new data with much small error bars are only in agreement with those calculations which treat the kaon potential in the covariant kaon dynamics. This indicates that it is necessary to include the in-medium kaon potential in order to describe the new data for the K^+ transverse flow.

From Fig. 6 it is seen that the strongly repulsive static potential tends to push the kaons dramatically away from the spectator matter, leading to a strong antiflow around midrapidity (stars). The effect of the LF contribution in the covariant kaon dynamics pulls the kaons back to the spectator matter, resulting in a finally reasonable pattern of the K^+ transverse flow, which is in good agreement with the FOPI data. This feature of the LF contribution can also be seen in Fig. 7 where the calculations are performed by the BRP with a hard EOS. This illustrates that the LF like contribution, originating from spatial components of the vector field, provides an important contribution to the in-medium kaon dynamics in heavy ion collisions. Kaons are produced in the early phase of the reaction where the relative velocity of projectile and target matter is large. Thus the kaons feel a nonvanishing baryon current in the spectator region, in particular in noncentral collisions. This contribution dramatically counterbalances the influence of the repulsive potential on the K^+ transverse flow.

From the comparison between the results in Figs. 6 and 7, on the other hand, it is found that the K^+ transverse flow calculated with a hard EOS gives rise to a slightly positive flow around midrapidity and a worse fit to the new data in the target region. This is due to the fact that the kaon in-medium potential calculated with a hard EOS is weaker than that given with a soft EOS (see Fig. 1). However, the K^+ transverse flow given with a hard EOS can also roughly describe the new data set within error bars. Thus it appears to

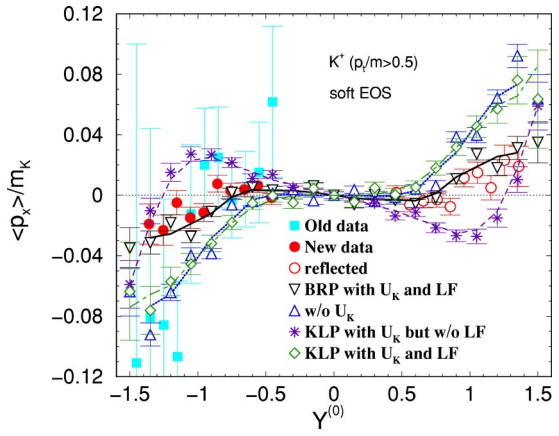

FIG. 8. (Color online) Same as shown in Fig. 6, but by the KLP with a soft EOS. Here the results by the BRP with U_K&LF are also shown.

be impossible to extract information on the nuclear EOS from the analysis of the K^+ side flow.

The K^+ transverse flow given by the KLP with a soft EOS is shown in Fig. 8 where the results by the BRP with U_K&LF for the soft EOS (open down triangles) are shown as well. In this figure the experimental data and their reflections with respect to midrapidity are represented by the same symbols as in Fig. 6. The results (stars) are calculated by the KLP with U_K but without (w/o) LF. The standard treatment with a static potential, Eq. (7), shows an antiflow around midrapidity which is larger than that given by the BRP with U_K&LF and is in better agreement with the old data. The situation changes, however, dramatically when the full Lorentz structure of the mean field is taken into account (diamonds). The influence of the repulsive potential of K^+'s on the in-plane flow is almost completely counterbalanced by the velocity dependent part of the interaction, i.e., the LF contribution. Hence, no net effect of the potential is any more visual. This is clearly seen from the comparison between this result (diamonds) and those (open up triangles) obtained without U_K. This seems to indicate that the static potential predicted by the KLP is too weak to overcome the cancellation effects of the LF on the flow. Using the BRP, the kaon in-medium potential has a stronger repulsive character which gives rise to a reasonably anticorrelated flow signal and leads to a good agreement with both, the old and new data set from FOPI.

In this context one has to keep in mind that the net source flow for the kaon production is experimentally not accessible. Here one has to rely on the predictions from transport models. The analysis of the small kaon flow signal which arises to large amount from the cancellation of large source flow components carries inherent uncertainties due to experimental and theoretical error bars of the source flow. Investigating the influence of the in-medium kaon potential we were confronted with two effects: If the kaon dynamics is described by the standard treatment with a static potential, i.e., neglecting the effect of a Lorentz force from spatial component of the vector field, the calculated K^+ in-plane flow is not able to reproduce the new FOPI data with reasonable precision. The Lorentz force effect is large and it changes the K^+ flow pattern qualitatively. We consider this qualitative result therefore as stable. Quantitative statement on the strength of the kaon potential have to be made more carefully. Since differences are most pronounced at large spectator rapidities where the experimental proton flow is within error bars well reproduced by the present transport calculations, the K^+ flow can help to distinguish between different models. However, due to the smallness of the signal and present theoretical and experimental error bars, definite quantitative statements require further investigations.

IV. CONCLUSIONS

In summary, the influence of the chiral mean field on the transverse flow of kaons in heavy ion collisions at SIS energy has been investigated within covariant dynamics. The kaons inside the nuclear medium are described as quasiparticles carrying effective masses and momenta. This accounts for the correct mass-shell properties of the particles inside the nuclear medium. A consequence of the covariant kaon dynamics is the appearance of a momentum dependent force proportional to the spatial components of the vector field which resembles the Lorentz force in electrodynamics. Although such Lorentz forces vanish in equilibrated nuclear matter they provide an essential contribution to the dynamics in the case of energetic heavy ion collisions. The influence of in-medium effects on the in-plane flow is counterbalanced to large extent by this additional contribution.

In the present studies two types of in-medium potentials with different parametrizations have been applied. Their influence on the K^+ in-plane flow has been discussed. Our theoretical results show that in the covariant dynamics the new FOPI data can be reasonably described using a parametrization proposed by Brown and Rho which partially accounts for higher-order corrections in the chiral expansion. The reproduction of the more recent FOPI data, in particular at spectator rapidities, requires a relatively strong repulsive K^+ potential, which is in good agreement with those determined from the kaon-nucleon scattering length using the impulse approximation [27] and also with recent information obtained from $p+A$ reactions [22]. This finding is consistent with the description of the K^+ multiplicities in $A+A$ reactions. Most transport simulations reproduce corresponding data [8] only when in-medium potentials are included [12,14,16,20]. In summary, information extracted from the analysis of the K^+ transverse flow is consistent with the knowledge from other sources.

ACKNOWLEDGMENTS

One of the authors (Y.M.Z.) was grateful to C. M. Ko for useful discussions. This work was supported in part by the National Natural Science Foundation of China (NSFC) under Grant Nos. 19975074 and 10275096, by the Deutsche Forschungsgemeinschaft (DFG) under Grant No. 446CHV-113/91/1, and by the National Research Concil of Thailand (NRCT) under Grant No. 1.CH7/2545.

[1] B. D. Kaplan and A. E. Nelson, Phys. Lett. B **175**, 57 (1986); A. E. Nelson and B. D. Kaplan, *ibid.* **192**, 193 (1987).
[2] G. E. Brown and M.Rho, Nucl. Phys. **A596**, 503 (1996).
[3] J. Schaffner, J. Bondorf, and I. N. Mishustin, Nucl. Phys. **A625**, 325 (1997).
[4] T. Waas, N. Kaiser, and W. Weise, Phys. Lett. B **365**, 12 (1996); T. Waas, M. Rho, and W. Weise, Nucl. Phys. **A617**, 449 (1997).
[5] M. Lutz, Phys. Lett. B **426**, 12 (1998).
[6] G. Q. Li, C.-H. Lee, and G. E. Brown, Nucl. Phys. **A625**, 372 (1997); Phys. Rev. Lett. **79**, 5214 (1997).
[7] J. L. Ritman and FOPI Collaboration, Z. Phys. A **352**, 355 (1995).
[8] D. Miskowiec *et al.*, KaoS Collaboration, Phys. Rev. Lett. **72**, 3650 (1994); Y. Shin, *et al.*, KaoS Collaboration, *ibid.* **81**, 1576 (1998); F. Laue, *et al.*, KaoS Collaboration, *ibid.* **82**, 1640 (1999).
[9] M. Menzel *et al.*, KaoS Collaboration, Phys. Lett. B **495**, 26 (2000).
[10] C. Sturm *et al.*, KaoS Collaboration, Phys. Rev. Lett. **86**, 39 (2001).
[11] D. Best *et al.*, FOPI Collaboration, Nucl. Phys. **A625**, 307 (1997).
[12] C. M. Ko, J. Phys. G **27**, 327 (2001); G. Q. Li, C. M. Ko, and Bao-An Li, Phys. Rev. Lett. **74**, 235 (1995); G. Q. Li, C. M. Ko, Nucl. Phys. **A594**, 460 (1995).
[13] C. M. Ko, G. Q. Li, J. Phys. G **G22**, 1673 (1996).
[14] E. L. Bratkovskay, W. Cassing, and U. Mosel, Nucl. Phys. **A622**, 593 (1997); Phys. Lett. B **424**, 244 (1998).
[15] C. David, C. Hartnack, and J. Aichelin, Nucl. Phys. **A650**, 358 (1999).
[16] C. Hartnack and J. Aichelin, J. Phys. G **G28**, 1649 (2002).
[17] Z. Wang, Amand Faessler, C. Fuchs, V. S. Uma Maheswari, and D. S. Kosov, Phys. Rev. Lett. **79**, 4096 (1997).
[18] Z. Wang, Amand Faessler, C. Fuchs, V. S. Uma Maheswari, and D. S. Kosov, Nucl. Phys. **A628**, 151 (1998).
[19] C. Fuchs, D. S. Kosov, Amand Faessler, Z. S. Wang, and T. Waindzoch, Phys. Lett. B **434**, 245 (1998); C. Fuchs, Amand Faessler, Z. S. Wang, and T.Gross-Boelting, Prog. Part. Nucl. Phys. **42**, 197 (1999).
[20] C. Fuchs, Amand Faessler, E. Zabrodin, and Y. M. Zheng, Phys. Rev. Lett. **86**, 1974 (2001).
[21] Y. M. Zheng, Z. L. Chu, C. Fuchs, Amand Faessler, W. Xiao, D. P. Hua, and Y. P. Yan, Chin. Phys. Lett. **19**, 926 (2002).
[22] M. Nekipelov *et al.*, COSY Collaboration, Phys. Lett. B **540**, 207 (2002).
[23] H. Herrmann and FOPI Collaboration, Prog. Part. Nucl. Phys. **42**, 187 (1999).
[24] B. D. Serot and J. D. Walecka, Adv. Nucl. Phys. **16**, 1 (1988).
[25] Y. M. Zheng, C. Fuchs, and Amand Faessler, High Energy Phys. Nucl. Phys. **26**, 77 (2002).
[26] X. S. Fang, C. M. Ko, G. Q. Li, and Y. M. Zheng, Nucl. Phys. **A575**, 766 (1994); Phys. Rev. C **49**, R608 (1994).
[27] G. E. Brown, C. H. Lee, M. Rho, and V. Thorsson, Nucl. Phys. **A567**, 937 (1994).
[28] T. Barnes and E. S. Swanson, Phys. Rev. C **49**, 1166 (1994).
[29] A. Sibirtsev, Phys. Lett. B **359**, 29 (1995).
[30] K. Tsushima, A. Sibirtsev, A. W. Thomas, and G. Q. Li, Phys. Rev. C **59**, 369 (1999).
[31] K. Tsushima, S. W. Huang, and A. Faessler, Phys. Lett. B **337**, 425 (1994); J. Phys. G **21**, 33 (1995).
[32] C. Sturm, Ph.D.thesis, TU Darmstadt, 2001.
[33] Z. Wang, Amand Faessler, C. Fuchs, and T. Gross-Boelting, Nucl. Phys. **A645**, 177 (1999); **A648**, 281(E) (1999).
[34] G. Q. Li and C. M. Ko, Phys. Rev. C **54**, 1897 (1996).